

# An Improved Family of Low Dispersion Finite Volume Schemes for Aeroacoustic Applications

Douglas V. Nance

USAF Wright Laboratory, Eglin AFB, FL

L. N. Sankar

School of Aerospace Engineering, Georgia Institute of Technology, Atlanta, GA

K. Viswanathan

Dynacs Engineering Company, Inc., Renton, WA

## Abstract

This paper describes the development of a second generation of low dispersion numerical schemes in the context of a finite volume discretization of the governing fluid dynamic equations. Until recently, finite volume methods had not been endowed with techniques designed to mitigate numerical dispersion errors. The purpose of this study is to present a new family of low dispersion finite volume numerical schemes, the Type 2 formulation. The Type 1 family of schemes was presented in an earlier work. As in any finite volume method, the surface integrals are computed by using flow field properties at the cell faces, interpolated from values stored at the cell nodes. The new family of schemes uses an interpolation procedure designed to optimize the difference in sinusoidal wave properties occurring across a given cell interface. This procedure renders a more accurate representation of the wave variable differences at higher wavenumbers. This new family of schemes is better suited for application in the flux difference splitting algorithms commonly found in computer programs designed for computational fluid dynamics. It is of particular interest that the new schemes mitigate numerical dispersion errors for both interface variables and for the differences in wave variables across a cell interface. A number of classical acoustics problems are solved, and where possible, comparisons with other numerical and exact solutions are shown. It is especially significant that this new method has low numerical dispersion and may be easily retrofitted into existing finite volume codes.

## Introduction

Improvements in propulsion and mechanical system design have resulted in significant reductions in aircraft noise emissions. As a result, flow-related aeroacoustic noise has become a prominent part of an aircraft's acoustic signature. To satisfy ever more stringent U.S. federal regulations governing radiated noise, computational aeroacoustics (CAA) research efforts have grown steadily. Today's CAA techniques have their origins beginning with the pioneering work of Rayleigh who defined and classified multi-pole acoustic emitters (Hessinius<sup>1</sup>). Later, Lighthill demonstrated the importance of quadrupole emitters to aeroacoustic noise and developed the widely applied acoustic analogy, a vital link between the nonlinear flow field and the linear acoustic farfield<sup>2</sup>. The analogy has been extended to incorporate solid surface effects through the work of Ffowcs Williams, Hall, and Howe<sup>3</sup>. Similar techniques employ Kirchoff's formulation and the use of Green's functions to calculate the acoustic field based on knowledge of the nonlinear flow field (Lyrintzis<sup>4</sup>). Still, in these early stages of research, solution of both the flow field and acoustic field relied upon the use of analytical models.

Now finite difference techniques are popular for use in simulating the aeroacoustic field. MacCormack's method has been applied to a number of classical aeroacoustic problems (Lim et al.<sup>5</sup>). A number of other finite difference schemes have been devised for computing linear acoustic waves (Thomas and Roe<sup>6</sup>). Still, the numerical solution of aeroacoustic problems presents certain technical difficulties, because acoustic waves are particularly susceptible to numerical dispersion and dissipation (Tam<sup>7</sup>). Classical dispersion-relation-preserving (DRP) finite difference schemes were devised to produce minimally dispersive solutions for acoustic wave problems (Tam and Webb<sup>8</sup>). Tam's excellent studies on classical DRP schemes have motivated the application of DRP principles to upwind methods.

Upwind schemes are gaining popularity in CAA research because of their ease of applicability to finite volume codes. Van Leer's third-order, Monotone Upwind Scheme for Conservation Laws (MUSCL) was applied to simple aeroacoustic problems in (Sankar et al.<sup>9</sup>). The same technique has also been used to predict propeller-induced acoustic levels (Lim et al.<sup>5</sup>). When applied as a high order method to aeroacoustic problems, no artificial smoothing is required to stabilize the scheme. However, the intrinsic damping in the upwind method does tend to "wash out" subtle acoustic waves (Tam<sup>7</sup>). This difficulty motivated the development of low dispersion finite volume (LDFV) schemes wherein Tam's ideas were extended to curvilinear geometries for the finite volume discretization method. The results for several test problems were presented for the Type 1 (T1) LDFV scheme (Nance et al.<sup>10</sup>). Below, an extension of this work is given. The Type 2 (T2) discretization is algebraically linked to the optimized differential operator stencil lending to improved dispersive and dissipative performance. It is further shown that

the T2 scheme collapses to Tam's classical DRP formulation on the uniform grid. A series of calculations are presented for problems taken from the first ICASE/LaRC Workshop on CAA. Preliminary results are also shown for the application of the T2 scheme to vortex shedding from a cylinder.

## Mathematical Formulation

### Finite Volume Form for a Hyperbolic PDE

Upwind schemes were devised for use in the solution of hyperbolic partial differential equations. In the case of aeroacoustic problems, the hyperbolicity arises due to the presence of differing characteristic wave speeds in the flow field. Consider the general form of a hyperbolic partial differential equation

$$\frac{\partial \vec{q}}{\partial t} + \frac{\partial \vec{F}}{\partial x} + \frac{\partial \vec{G}}{\partial y} = 0. \quad (1)$$

For efficiency of notation, we have shown the two-dimensional form where  $\vec{q}$  is the vector of conservative variables and  $\vec{F}$  and  $\vec{G}$  are flux vectors. Equation (1) may be written for scalar quantities as well. In order to apply upwinding to (1), we use the quasilinear form

$$\frac{\partial \vec{q}}{\partial t} + \frac{\partial(A\vec{q})}{\partial x} + \frac{\partial(B\vec{q})}{\partial y} = 0, \quad (2)$$

where A and B are the flux Jacobian matrices. By using Hardin's flow/acoustic splitting<sup>11</sup>, we assume that  $\vec{q}$  can be represented by the sum of a main flow field variable  $\vec{q}_0$  and an acoustic variable  $\vec{q}$ , i.e.,

$$\vec{q} = \vec{q}_0 + \vec{q}. \quad (3)$$

Suppose that  $\vec{q}$  is only a small perturbation; if so, (2) and (3) imply that

$$\frac{\partial \vec{q}}{\partial t} + \frac{\partial(A_0\vec{q})}{\partial x} + \frac{\partial(B_0\vec{q})}{\partial y} = 0, \quad (4)$$

where  $A_0$  and  $B_0$  depend solely upon the properties of the main flow field. As a result, (4) describes the variation of the linear acoustic field as impacted by the flow field. Equation (4) is in divergence form, so it may be integrated over an arbitrary control volume to obtain

$$\frac{\partial}{\partial t} \int_V \vec{q} dV + \oint_{\partial(V)} (A_0 \hat{i} + B_0 \hat{j}) \vec{q} \cdot \hat{n} dS = 0. \quad (5)$$

In equation (5), the primes have been dropped for brevity, and  $\partial(V)$  denotes the boundary of  $V$ . By using a similarity transformation as given in (Hirsch<sup>12</sup>), on the matrix sum in (5), we may write the upwinded form

$$(A_0 \hat{i} + B_0 \hat{j}) \cdot \hat{n} = \hat{A}^+ + \hat{A}^-. \quad (6)$$

Then by applying (5) and (6) to a trapezoidal grid cell, we have

$$\frac{d}{dt} (\vec{q} V_{cell}) = \vec{R}_{cell}, \quad (7)$$

with

$$\vec{R}_{cell} = - \sum_{m=1}^4 (\hat{A}^+ \vec{q}_L + \hat{A}^- \vec{q}_R)_{cell}^m \Delta S_{cell}^m, \quad (8)$$

where  $V$  is the cell area;  $\Delta S$  is the length of the  $m^{th}$  cell face, and  $\vec{q}_L$  and  $\vec{q}_R$  are the upwind values of  $\vec{q}$  taken to the left and right of the  $m^{th}$  cell face, respectively.

### The Classical DRP Scheme

To provide a smooth introduction to LDFV schemes, we must first discuss the classical DRP scheme of Tam and Webb<sup>8</sup>. This method offers a high accuracy stencil representation for a first order space derivative, say  $\frac{\partial u}{\partial x}$ . As with standard finite differences, such a derivative may be represented using the uniform, symmetric stencil

$$\frac{\partial u(x_i)}{\partial x} = \frac{1}{\Delta x} \sum_{k=-M}^M a_k u(x_i + k\Delta x), \quad (9)$$

where the  $a_k$  are fixed coefficients. The  $a_k$  are chosen to satisfy an order of accuracy and to match the dispersion relation for  $\frac{\partial u}{\partial x}$ . By taking Fourier transforms in (9), we can derive a relationship between the numerical and actual wavenumber/mesh size products  $\alpha \Delta x$ , i.e.,

$$(\alpha\Delta x)_{num} = -i \sum_{k=-M}^M a_k \exp(ik\alpha\Delta x). \quad (10)$$

We obtain an algebraic equation for  $a_j$  by minimizing, in the sense of least squares, the difference

$$d(\alpha\Delta x, a_j) = \|(\alpha\Delta x)_{num} - \alpha\Delta x\|^2,$$

for  $\alpha\Delta x$  integrated over the range  $-\frac{\pi}{2} \leq \alpha\Delta x \leq \frac{\pi}{2}$ .

### The LDFV Schemes

The purpose of the LDFV method is to combine the flexibility of upwind schemes with the numerical dispersion reduction capabilities of classical DRP schemes. The T1 LDFV scheme was developed by representing a cell face variable with the stencil

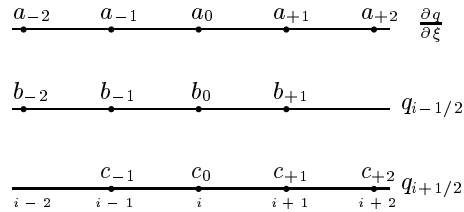
$$q_{i+1/2} = \sum_{k=-M}^N a_k q(\xi_{i+1/2} + \Delta_k \xi), \quad (11)$$

where the  $\Delta_k \xi$  are the distances from  $\xi_{i+1/2}$  to  $\xi_k$ . Note that the stencil described by ( 11) is, in general, asymmetric. The Fourier transform of ( 11) was taken, and a least-squares minimization was performed to render a system of equations for the  $a_k$  marked by minimal dispersion<sup>10</sup>. One such relation was combined with a set of equations for establishing the order of accuracy of  $q_{i+1/2}$ . The solution of this system of algebraic equations produced the  $a_k$ . For the T2 scheme, it is our goal to not only minimize dispersion for cell face variables, but to minimize the dispersion for cell interface variable differences as well. We can derive the T2 scheme by recognizing a stencil-based approximation for the derivative in the uniform computational grid, i.e.,

$$\frac{\partial q}{\partial \xi} \approx \frac{q_{i+1/2} - q_{i-1/2}}{\Delta \xi}. \quad (12)$$

Both  $q_{i+1/2}$  and  $q_{i-1/2}$  can assume asymmetric representations on the symmetric stencil used for  $\frac{\partial q}{\partial \xi}$ . Consider Figure 1 for the 5-point derivative stencil.

Figure 1: Stencil Decomposition



By using variants of equations ( 9), ( 11), and ( 12), we can write that

$$\frac{1}{\Delta \xi} \left[ \sum_{k=-1}^2 c_k q(\xi_{i+1/2} + \Delta_k \xi) - \sum_{j=-2}^1 b_j q(\xi_{i-1/2} + \Delta_j \xi) \right] = \frac{1}{\Delta \xi} \sum_{m=-2}^2 a_m q(\xi_i + m\Delta \xi). \quad (13)$$

When simplified, ( 13) provides an underdetermined system of equations involving the  $b_k$  and the  $c_k$  in terms of the  $a_k$ . As it turns out, this system can be made determinate by enforcing order of accuracy constraints on either the left or the right upwind formula. For example, consider

$$q(\xi_{i+1/2}) = \sum_{k=-1}^2 c_k q(\xi_{i+1/2} + \Delta_k \xi). \quad (14)$$

By applying a Taylor series analysis to ( 14), we can derive a separate algebraic constraint on the  $c_k$  for each order of accuracy, zero or greater. It can be shown that this system becomes fully determinate while granting second order accuracy. The resulting  $c_k$  are given below in comparison with Van Leer's third order MUSCL scheme.

$c_k$	<u>LDFV T2</u>	<u>MUSCL</u>
$c_0$	0.391655	0.333333
$c_1$	0.716689	0.833333
$c_2$	-0.108344	-0.166667

For a five point T2 scheme, the real and imaginary parts of the dispersion relation are plotted in Figures 2 and 3. The ‘‘Taylor’’ curves result from analyzing the dispersion relation for the upwind formula derived from the standard symmetric difference formula for  $\frac{\partial q}{\partial \xi}$ .

## Results and Discussion

### The Linear Wave Equation in One Dimension

In this test case, we study the ability of our numerical scheme to convect a linear acoustic pulse without distortion. This problem is scalar in the acoustic quantity  $u$ , and exists in only one dimension  $x$ . The quantity  $u$  is initialized at  $t = 0$  with the Gaussian shape given below. For correct linear acoustic convection, the pulse should propagate along the  $x$ -axis in the positive direction with unit speed. Also, the actual shape of the pulse should remain unchanged with time. To obtain the linear wave equation in one dimension, we denote  $\vec{q}$  as scalar in equation ( 1) such that

$$q = F = u(x, t); \quad G = 0.$$

The initial conditions are given as

$$u(x) = \frac{1}{2} \exp\left(-\ln(2) \left(\frac{x}{3}\right)^2\right), \quad t = 0.$$

The chosen stepsizes are  $\Delta x = 1.0$  and  $\Delta t = 0.001$ . The solution is given at time 100 in Figure 4. The agreement between numerical and exact solutions is excellent, especially when the magnitude of the spatial stepsize is taken into account.

### The Spherical Wave Equation

This problem models the acoustic velocity field generated by a particular monopole, a type of spherical source. The sound generator is a sphere with a mean radius of five units. The surface of the sphere creates sound by oscillating in time with a radial velocity, given below, that is uniform over the sphere’s surface. The resulting spherical wave should decrease in amplitude, but retain its overall shape, as the wave propagates outward from the sphere. The spherical wave equation is obtained by again denoting  $\vec{q}$  as a scalar and by writing equation ( 1) with  $x = r$  and

$$q = F = ru(r, t); \quad G = 0.$$

This test case takes the form of a boundary value problem where

$$u(r, t) = 5 \cos(\omega t), \quad \omega = \frac{\pi}{4}.$$

The stepsizes selected are  $\Delta r = 1.0$  and  $\Delta t = 0.01$ . The time 200 solution is given as Figure 5. As was seen with the solution of the linear wave equation, the agreement between exact and numerical solutions is excellent.

### Reflection of an Acoustic Pulse off a Wall in the Presence of a Uniform Flow in Semi-Infinite Space

This test case is particularly interesting, because it involves the interaction of a convecting acoustic pulse with a rigid wall. The rigid wall is infinite in extent along the  $x$ -axis. The flow field is semi-infinite for  $y > 0$ , and the flow convects in the positive  $x$  direction uniformly at Mach 0.5. At time zero, an acoustic pulse is initiated 25 units above the surface of the wall. The initial density and pressure relations have Gaussian profiles in  $x$  and  $y$  as given below. During the evolution of the acoustic field, the pulse should spread outward in a linear manner while convecting downstream. The pulse should also reflect properly from the rigid wall. To obtain the governing equations for this problem, a form of the linearized Euler equations, we substitute

$$\vec{q} = \begin{bmatrix} \rho \\ u \\ v \\ P \end{bmatrix}; \quad \vec{F} = \begin{bmatrix} M_x \rho + u \\ M_x u + P \\ M_x v \\ M_x P + u \end{bmatrix} \quad \vec{G} = \begin{bmatrix} v \\ 0 \\ P \\ v \end{bmatrix}$$

in equation ( 1). For this test case,  $M_x = 0.5$ . The initial conditions are given as

$$P = \rho = \exp\left[-\ln(2) \left(\frac{x^2 + (y-25)^2}{25}\right)\right]; \\ u = v = 0.$$

The stepsizes selected are  $\Delta x = \Delta y = 1.0$  and  $\Delta t = 0.25$ . The numerical solution is shown at time 75 in Figure 6. The agreement with the exact solution is quite good, but more importantly, the quality of the numerical solution improves with time. This characteristic of the numerical solution is very desirable for CAA schemes.

### Vortex Shedding from a Cylinder in Uniform Flow

This section is designed to present preliminary results for a time-accurate numerical simulation of the shedding of vortices from an infinite cylinder immersed in a uniform, compressible flow. The unsteady pressure and velocity fields generated by the shedding vortices create noise. In this case, the laminar Navier-Stokes equations are solved in conservative form for a cylinder of unit diameter. The freestream Mach number is 0.2, and the Reynolds number is 200. Ultimately, the acoustic perturbations are to be extracted from points in the farfield and then analyzed for spectral content. A plot of the flowfield is shown in Figure 7; vortices can be seen shedding from the cylinder. The T2 scheme is used in this nonlinear simulation to provide the left and right cell interface variables. The pressure and velocity fluctuations caused by the continuous shedding of vortices cause the emission of acoustic waves that travel upstream and downstream in this flow. This simulation can also be performed on large grids and at higher Reynolds numbers.

### Conclusions

A second family of low dispersion finite volume schemes has been described. The first derivative as discretized by the Type 2 low dispersion finite volume scheme has been shown to be equivalent to the classical DRP discretization. This new scheme has also proven to mitigate numerical dispersion errors for both the cell face variables and for their interface differences. In most cases, the Type 2 scheme provides decidedly better numerical solutions than the Type 1 scheme. It has also been shown that the low dispersion finite volume schemes are readily usable for the simulation of nonlinear problems such as vortex shedding from a cylinder.

### References

- (1) Hessinius, K., Welcome Address in *Computational Acoustics*. Hardin, J.C. and Hussaini, M.Y., eds., Springer-Verlag, New York, 1993.
- (2) Lighthill, J., Keynote Address in *Computational Acoustics*. Hardin, J.C. and Hussaini, M.Y., eds., Springer-Verlag, New York, 1993.
- (3) Howe, M.S., "A review of the theory of trailing edge noise", *J. of Sound and Vibration*, Vol. 61, No. 3, pp. 437-465, 1978.
- (4) Lyrintzis, A.S., "Review: the use of Kirchoff's method in computational aeroacoustics", *J. Fluids Engineering*, Vol. 116, pp. 665-676, 1994.
- (5) Lim, T.B., Sankar, L.N., Hariharan, N., and Reddy, N.N., "A first principle based technique for propeller noise problem", AIAA Paper 93-4340.
- (6) Thomas, J.P. and Roe, P.L., "Development of non-dissipative numerical schemes for computational aeroacoustics", AIAA Paper 93-3382, 1993.
- (7) Tam, C.K.W., "Computational aeroacoustics: issues and methods", *AIAA Journal*, Vol. 33, No. 10, pp. 1788-1796, 1995.
- (8) Tam, C.K.W. and Webb, J.C., "Dispersion- relation-preserving schemes for computational acoustics", *J. Computational Physics*, Vol. 107, pp. 262-281, 1993.
- (9) Sankar, L.N., Reddy, N.N., Hariharan, N., "A third order upwind scheme scheme for aeroacoustic problems", AIAA Paper 93-0149, 1993.
- (10) Nance, D.V., Viswanathan, K., and Sankar, L.N., "A low dispersion finite volume numerical scheme for aeroacoustic applications", AIAA Paper 96-0278, 1996.
- (11) Hardin, J., Invited lecture given at the ASME Forum on Computational Aeroacoustics and Hydroacoustics, 1993.
- (12) Hirsch, C., Numerical Computation of Internal and External Flows. Vol. 2, John Wiley & Sons, New York, 1988.

### Acknowledgements

The second author was supported by the National Rotorcraft Technology Center under the CERT program.